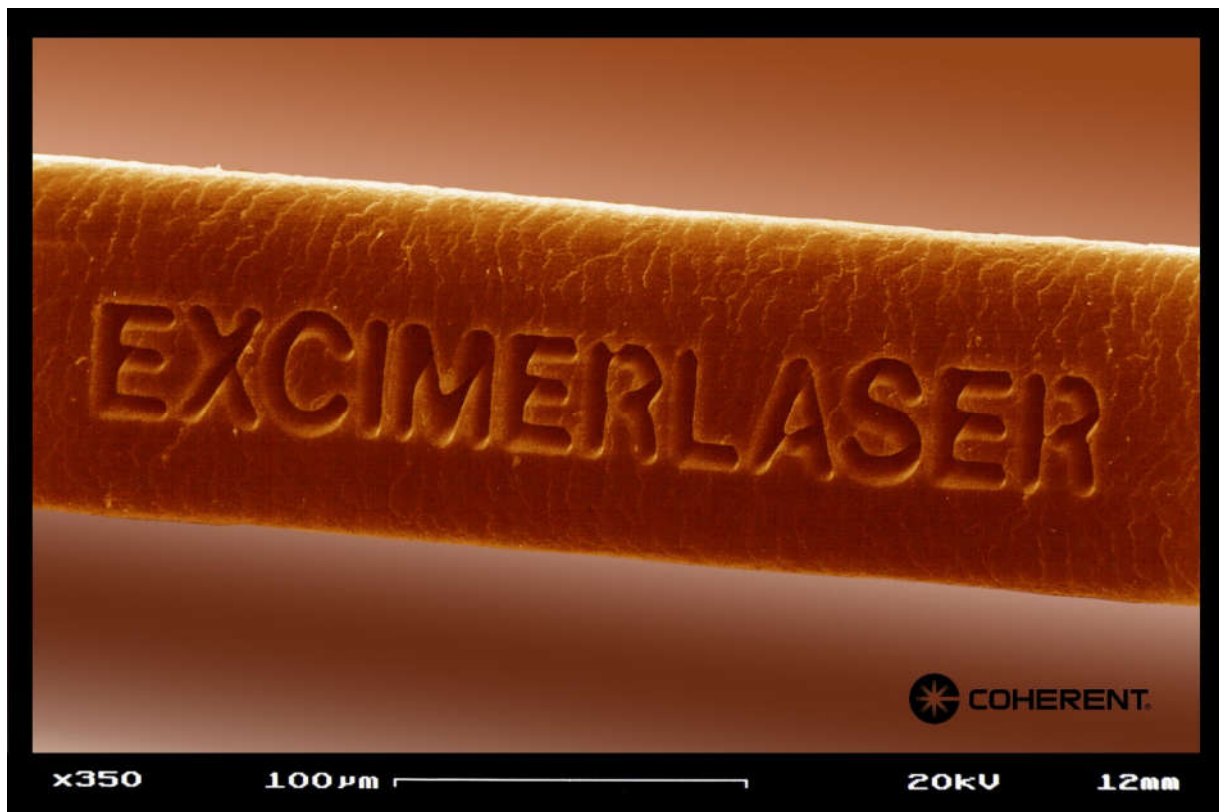




## Ablation of BioPolymers with 193 nm Excimer Pulses

There is increasing interest in precision micromachining and patterning of biopolymer substrates and films, in part for use as biodegradable fibers and waveguides for novel medical procedures based on deep tissue laser delivery. However, this structuring is challenging because these biopolymers are often thermo-mechanically delicate. Here we discuss results from a research study that successfully utilized pulses from a Coherent 193 nm excimer laser to create optical structures in the polymer chitosan.





## Biopolymers – Potential Photonic Applications

Polymers that are bio-derived and biodegradable have long been used in medicine because they are naturally absorbed by the body (bio-absorbed) over time. This makes them well-suited for procedures requiring implantation without the complication of eventual retrieval. Of course, the simplest and oldest examples are the fibers used for bio-absorbable sutures for internal wound closure. More recently, these types of polymers are attracting particular interest for use as bio-absorbable photonic components, such as fibers and waveguides. Here the overarching goal is to be able to deliver therapeutic laser light deep into tissue. The need arises because light is strongly absorbed and scattered by tissue, limiting its penetration to a few millimeters or even just micrometers, depending on the wavelength. As a result, while lasers are the dominant tools for many aesthetic procedures that target the dermis and sub-dermis, they are less widely used for cutting internal tissues.

Limited penetration depth is the reason that fiber delivery is a key consideration when developing new laser surgical techniques. For example, a new thulium laser from Coherent at a wavelength of 2  $\mu\text{m}$  can be transmitted via glass fiber, and is already being investigated for micro-surgical procedures targeting neurological tumors with limited accessibility.

However, if the light can be delivered via a sacrificial bio-absorbable device, then the range of potential laser-based treatment options can be greatly expanded, including treatments that require repeated laser irradiation. For example, a recently published study showed the ability to close deep (>10 mm) wounds in porcine skin via a laser-based technique called photochemical tissue bonding (PTB) using planar waveguides fabricated from polylactic-type biopolymers.

## Chitosan Films Spun on Glass

Chitosan is a transparent polymer derived from the shells of shrimp and other arthropods. It is a natural polymer ( $\beta$ -1,4-linked 2-amino-2-deoxy-D-glucopyranose) that is used in medical applications including drug delivery, antimicrobial applications, and tissue engineering. There are many methods used to pattern chitosan, such as nano-imprint lithography, ion beam milling and laser ablation processing. And, there are literature reports regarding the successful creation of optical structures, including waveguides and diffraction gratings.

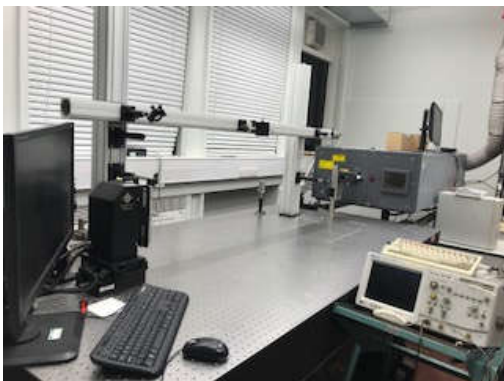


**Figure 1.** The laser beam delivery system used in this ablation study with the 193nm excimer laser.



If laser ablation is to be used for commercial production of implantable photonic devices based on chitosan, a critical factor will be a thorough understanding of the laser/material interaction. This is necessary in order to optimize the process for various applications, and to establish process windows for these purposes. Since chitosan is transparent with no absorption in the visible spectrum, laser ablation must be performed with ultraviolet laser sources. In fact, laser ablation of chitosan had previously been investigated using the 248 nm output of a KrF excimer laser, but with rather limited results. (248 nm laser ablation was found to be characterized by undesirable foaming). Here we describe the first reported detailed study on the interaction of deep UV pulses from a 193 nm excimer with thin chitosan films, including practical data and comprehensive theoretical analysis. This work also includes the creation of grating-like patterns as would be required in laser delivery devices.

There are numerous methods to produce chitosan in various forms, e.g., films and spheres. The samples used in this study were created using an established spin coating method to create thin films on soda-lime glass slides. The spin process was adjusted to produce films at various thicknesses from 500 nm to 10  $\mu\text{m}$ . The films were conventionally air dried prior to the laser ablation experiments.

The ablation setup was based on a Coherent LPF 202 excimer laser emitting at a wavelength of 193 nm shown by figure 1. The laser output passed through a dual rotating plate attenuator (MetroLux, ML2110) to control the laser fluence. A stainless steel circular object mask of 2 mm diameter was positioned in a uniform part of the raw laser beam. The aperture was imaged onto the free surface of the chitosan using a 1:10 reduction. Surface metrology was performed using a Scanning Electron Microscope (SEM) and a White Light Interferometer (WLI).

The aim was to perform a comprehensive study and analysis of the laser-chitosan interaction at a wavelength of 193 nm, where very little work had previously been reported. For example, there wasn't even a published value for the chitosan ablation threshold at this deep UV wavelength. The 193 nm excimer was identified as a highly promising candidate ablation source for several reasons. First, the short wavelength minimizes diffraction and so can enable patterning of substrates with high spatial resolution. Second, just as important, the VIS-UV absorption spectrum was measured for chitosan films spun on fused silica slides, and confirmed that the absorption increases rapidly with decreasing wavelength below 225 nm. High absorption translates into short penetration depth, providing the highest possible depth control of any features ablated into these films. And third, an initial theoretical analysis showed that the measured pulse width of the ArF laser (11.5 ns) was compatible with ablating chitosan without unwanted thermal- and pressure-induced peripheral damage to the surrounding material.

### **Pulsed Laser Ablation – Theoretical Analysis**

The experimental study was complemented with calculations of the thermal and stress gradients and waves, including performing simulations of how these would arise and dissipate based on different laser pulse intensities and film thicknesses. It is well-known that if the absorbed energy from a laser pulse is deposited so rapidly that the heat does not have time to relax and diffuse out of the ablation volume, then a condition called thermal confinement arises, where peripheral thermal damage is virtually absent; most of the laser pulse energy is carried away in the ablated material. This condition can be formalized in terms of the thermal diffusivity, where the criterion for thermal confinement is



that the laser pulse duration has to be shorter than a characteristic thermal relaxation time ( $\tau_{th}$ ), as given by:

$$\tau_{th} = d^2/4\chi$$

Where  $d$  is the shortest distance within the irradiated volume, either the spot size or the optical absorption depth, and  $\chi$  is the thermal diffusivity. For many biological tissues and natural polymers the thermal diffusivity is low (typically  $10^{-8}/m^2/s$ ). So assuming a similarly low value for chitosan, a pulse width of several nanoseconds was predicted to be sufficiently short to ensure no peripheral damage such as thermal denaturation.

The impact of acoustic stress was also considered. The recoil energy from even small amounts of expelled material can lead to significant stresses and contribute to further material removal via a photo-acoustic mechanism. This type of mechanism has been widely reported for laser ablation of biological tissue and polymeric materials. It occurs when the laser pulse duration,  $\tau_p$ , is shorter than the acoustic relaxation time,  $\tau_{ac}$ . Under this condition, a stress confinement situation occurs. In simple terms, the irradiated material does not have sufficient time to reconfigure by changing its volume and consequently there is an abrupt increase in internal pressure. A compressional wave results, which creates a tensile wave. This may lead to bond breakage, cavity formation and bubble nucleation. In some cases, depending on the laser fluence, heat may also be generated leading to laser induced material damage. For these reasons, the temperature rise was modeled and mapped based on different laser fluences. The temperature was calculated from analytical heat transfer equations.

The thermal decomposition process in these chitosan thin film samples was also measured using a process called thermogravimetric analysis. This showed that chitosan undergoes thermal decomposition at  $\sim 300^\circ C$ . It is therefore very important that any substrate heating due to the ablation process must not result in temperatures approaching this value if thermal damage is to be avoided. Figure 2 shows the temperature rise for chitosan that has been irradiated using a laser fluence of  $80 \text{ mJ}/\text{cm}^2$  and  $760 \text{ mJ}/\text{cm}^2$  respectively. At the lower laser fluence, the temperature rise is relatively low:  $\sim 40^\circ C$ . However, at a higher laser fluence of  $760 \text{ mJ}/\text{cm}^2$ , there is a significant increase in the temperature rise, reaching  $\sim 385^\circ C$  at the front surface of the chitosan.

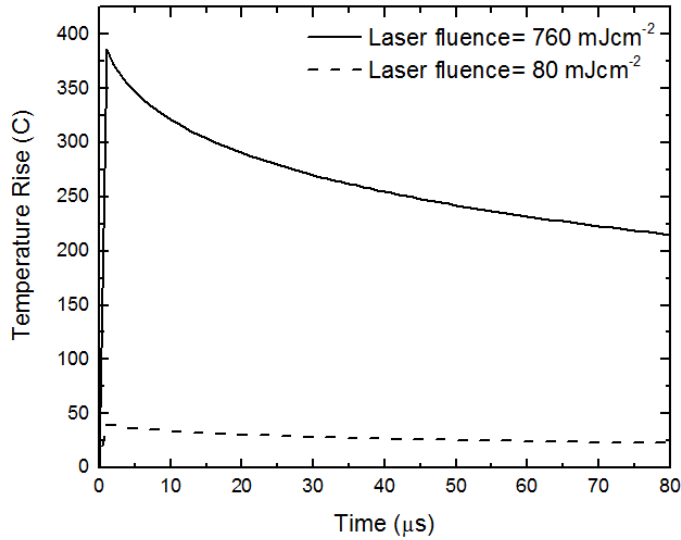


**Figure 2.** The temperature rise of irradiated chitosan films, at two different laser fluences.

### Ablation Results

One of the first experimental tasks was to determine the laser ablation threshold at 193 nm. This was accomplished by performing a series of etch rate measurements over a laser fluence range from 70 mJ/cm<sup>2</sup> to a maximum of 4.5 J/cm<sup>2</sup>. Etch depths were established by measuring the depths of the ablation craters using a White Light Interferometer (WLI). From these measurements, an ablation threshold of  $FT = 80 \pm 10$  mJ/cm<sup>2</sup> was extrapolated as shown in figure 3. As expected, ablation etch rates close to the ablation threshold were very low, at the nanometer/pulse level. Above 100 mJ/cm<sup>2</sup>, the etch rate increased very rapidly until about 120 mJ/cm<sup>2</sup>, where the etch rate began to plateau. This plateau effect is possibly due to changes in reflectivity due to locally dense vapor plume, which is common in many laser ablation processes. However, it may also be caused by surface topography changes.

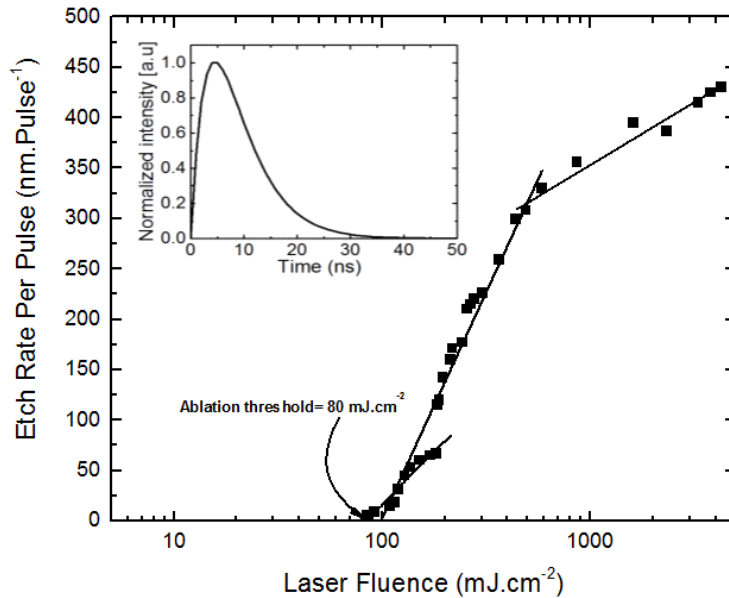


**Figure 3.** Etch rate measurements of laser ablated chitosan at a wavelength of 193 nm. The inset shows the measured temporal laser pulse,  $\tau_p = 11.5$  ns FWHM.

The experimentally determined ablation threshold was compared with a simple thermal energy balance equation:

$$\alpha F_{\text{evap}} = \rho [C(T_b - T_0) + L_v]$$

where  $C$  is the specific heat capacity,  $T_b$  and  $T_0$  are the boiling temperature and initial temperature respectively,  $\rho$  is the density, and  $L_v$  is the latent heat of vaporization. This predicts an ablation threshold of  $F_{\text{evap}} = 900$  mJ/cm<sup>2</sup>. This is ten times greater than the observed value. A probable explanation for this large difference is that the ablation process is not primarily photothermal, but instead dominated by photoacoustic effects. This interpretation is supported by SEM images of the ablated surface quality at an ablation fluence close to threshold, namely 95 mJ/cm<sup>2</sup>. As can be seen in figure 4, there is localized blistering of the surface, indicative of sub-surface material transformation. It is possible that this blistering could be due to inhomogeneities in the projected laser beam or the chitosan films. Indeed, the preparation of chitosan films from solution is a somewhat stochastic process. This is confirmed by the spread in literature values for the glass transition temperature of chitosan created from solution:  $T_g$  values vary from 140°C to 203°C.

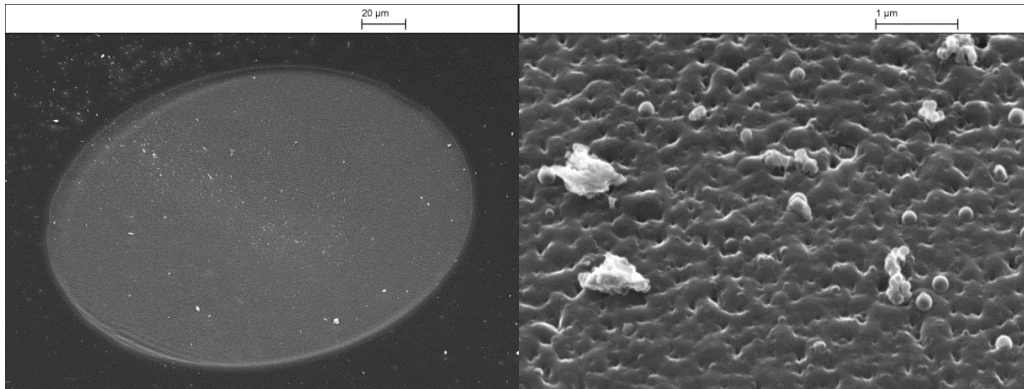


**Figure 4.** (left) SEM image of chitosan thin film in thickness of  $2.7\ \mu\text{m}$  irradiated with  $193\ \text{nm}$  laser, imaged in  $10\times$  magnification, repetition rate  $1\ \text{Hz}$ , 10 laser pulses, laser fluence  $95\ \text{mJ}/\text{cm}^2$ , depth  $4.5\ \text{nm}$  per pulse, circle mask of  $2\ \text{mm}$  diameter, tilt angle  $45^\circ$  and at a magnification of  $1.6\text{k}$ . (Right) the same parameters as above and at a  $60\text{k}$  magnification.

At much higher fluences (e.g.,  $250\ \text{mJ}/\text{cm}^2$ ), the ablated surface shows foaming. This has been reported for laser ablation of other biopolymers (e.g., collagen) and is suspected to be further evidence here of sub-surface photoacoustic effects. Turning to possible photonic applications, several different ablation patterns were then created. Here the ability to precisely control the etch depth meant that both amplitude and phase gratings could be created. A typical example of these patterns is the cross grating structure shown in figure 5. This is a small section of a large area ( $5\ \text{mm} \times 5\ \text{mm}$ ) cross grating structure imaged with the WLI. This was created by complete ablation of a nominal  $500\ \text{nm}$  film of chitosan, where the material between the mesas is etched down to the glass. The ablation was performed with a fluence of  $110\ \text{mJ}/\text{cm}^2$  and the SEM images indicate there is no significant thermal damage at this low fluence.

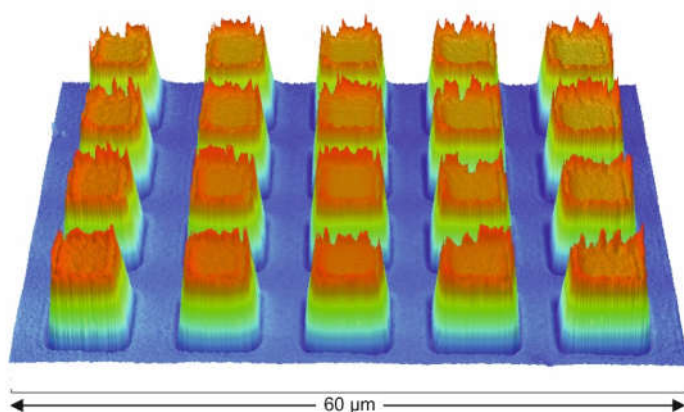


**Figure 5.** White light Interferometric (WLI) measurement of laser irradiated chitosan. The square structures are  $10\ \mu\text{m}$  square and  $525\ \text{nm}$  high. The structure was produced by mask projection and translating the sample relative to the beam using a laser fluence  $110\ \text{mJ}/\text{cm}^2$ , at a pulse repetition frequency of  $10\ \text{Hz}$ , a stage velocity of  $0.1\ \text{mm}/\text{s}$  and receiving 40 overlapping laser pulses.



## Summary

In conclusion, chitosan and other biopolymers have clear potential as photonic devices for use in novel medical procedures based on laser light. But actual implementation of these techniques will require precise patterning at the micron level. The deployment of laser ablation certainly shows promise for this application, but requires a thorough characterization of the laser/material interaction.

## World-leading excimer laser excellence

At Coherent excimer laser and adapted UV optical system designs are manufactured on 21,000 sqm production area in Göttingen, Germany. Cleanroom Class 7 (DIN EN ISO 14644) excimer laser tube manufacturing infrastructure as well as quality accreditation: ISO 9001/2008 certified and ISO 13485 certified, Lean and Six Sigma quality management in conjunction with build-to-order production supports highest levels of customization for industrial key customers and scientific users.



## Authors

Abdulsattar Aesa and Dr. Christopher Walton, University of Hull

[A.Aesa@2013.hull.ac.uk](mailto:A.Aesa@2013.hull.ac.uk); [c.d.walton@hull.ac.uk](mailto:c.d.walton@hull.ac.uk)

Ralph Delmdahl, Coherent Inc.; [Ralph.Delmdahl@coherent.com](mailto:Ralph.Delmdahl@coherent.com) – [www.coherent.com](http://www.coherent.com)





Special thanks to the University of Hull, Dr. Walton and his team!



Qassim Al-Jarwany	PhD student	Right
Dr. Christopher D. Walton	Supervisor	Middle
Abdulsattar Aesa	PhD student	Left